Molecular Microbiology (2008) 70(6), 1408–1423 ■
doi:10.1111/j.1365-2958.2008.06489.x
First published online 28 October 2008

# Regulation of glutamate metabolism by protein kinases in mycobacteria

**Helen M. O'Hare,[1,2]* Rosario Durán,[3] Carlos Cerveñansky,[3] Marco Bellinzoni,[4] Anne Marie Wehenkel,[4] Otto Pritsch,[5] Gonzalo Obal,[5] Jens Baumgartner,[1] Jérome Vialaret,[6] Kai Johnsson[1] and Pedro M. Alzari[4]****

[1]*Institute of Chemical Sciences and Engineering, Ecole Polytechnique Fédérale de Lausanne (EPFL), CH-1015 Lausanne, Switzerland.*
[2]*Departments of Infection, Inflammation and Immunity, and Biochemistry, University of Leicester, Leicester LE1 9HN, UK.*
[3]*Unidad de Bioquímica Analítica, Institut Pasteur de Montevideo/Instituto de Investigaciones Biológicas Clemente Estable, Uruguay.*
[4]*Unité de Biochimie Structurale (URA 2185 CNRS), Institut Pasteur, Paris, France.*
[5]*Unidad de Biofísica de Proteínas, Institut Pasteur de Montevideo, Uruguay.*
[6]*Proteomics core facility, Ecole Polytechnique Fédérale de Lausanne (EPFL), CH-1015 Lausanne, Switzerland.*

## Summary

**Protein kinase G of *Mycobacterium tuberculosis* has been implicated in virulence and in regulation of glutamate metabolism. Here we show that this kinase undergoes a pattern of autophosphorylation that is distinct from that of other *M. tuberculosis* protein kinases characterized to date and we identify GarA as a substrate for phosphorylation by PknG. Autophosphorylation of PknG has little effect on kinase activity but promotes binding to GarA, an interaction that is also detected in living mycobacteria. PknG phosphorylates GarA at threonine 21, adjacent to the residue phosphorylated by PknB (T22), and these two phosphorylation events are mutually exclusive. Like the homologue OdhI from *Corynebacterium glutamicum*, the unphosphorylated form of GarA is shown to inhibit α-ketoglutarate decarboxylase in the TCA cycle. Additionally GarA is found to bind and modulate the activity of a large $NAD^+$-specific glutamate dehydrogenase with an unusually low affinity for glutamate. Previous reports of a defect in glutamate metabolism caused by *pknG* deletion may thus be explained by the effect of unphosphorylated GarA on these two enzyme activities, which may also contribute to the attenuation of virulence.**

Accepted 1 October, 2008. For correspondence. *E-mail hmo7@le.ac.uk; Tel. (+44) 116 252 5089; Fax (+44) 116 252 5030; **E-mail alzari@pasteur.fr; Tel. (+33) 1 45 68 86 07; Fax (+33) 1 45 68 86 04.



## Introduction

*Mycobacterium tuberculosis*, the human pathogen responsible for tuberculosis, has a complex life cycle that comprises active extracellular and intracellular replicating forms as well as dormant states. The source of nutrients for mycobacteria at various stages of infection is not well defined, although the macrophage phagosome is presumed to be nutrient-poor (Munoz-Elias and McKinney, 2006). The classical prokaryotic mechanism for detection and response to environmental change is the two-component system, but serine/threonine (S/T) and tyrosine protein kinases and phosphatases are also widespread in prokaryotes. Notably, the number of S/T protein kinases in the genome of *M. tuberculosis* is equal to the number of complete two-component systems, and phosphorylation on S/T is thought to play a major role in signal transduction in this pathogen (Wehenkel *et al.*, 2008).

Among the 11 S/T protein kinases, PknG is of special interest as it may be directly involved in mycobacterial pathogenesis (Cowley *et al.*, 2004; Walburger *et al.*, 2004), but until now no substrate had been identified. The kinase activity has previously been studied using the surrogate substrate myelin basic protein or by measuring autophosphorylation (Koul *et al.*, 2001; Cowley *et al.*, 2004). In infected macrophages, PknG was proposed to be secreted into the cytosol, where this kinase was suggested to inhibit phagosome–lysosome fusion and promote intracellular survival of *M. tuberculosis* (Walburger *et al.*, 2004). Furthermore, inactivation of the *pknG* gene by allelic exchange decreases *M. tuberculosis* viability *in vitro* and causes delayed mortality of highly susceptible mice infected with this pathogen (Cowley *et al.*, 2004). The gene encoding PknG is part of a putative operon, conserved among mycobacteria and closely related actinomycetes, which also encodes proteins involved in glutamine uptake. A direct role for PknG in the regulation of glutamate metabolism is controversial in

mycobacteria (Cowley *et al*., 2004; Nguyen *et al*., 2005), but was clearly demonstrated for the related actinomycete *Corynebacterium glutamicum* (Niebisch *et al*., 2006). In this organism PknG was shown to regulate metabolism via phosphorylation of OdhI. In the unphosphorylated form, OdhI binds with high affinity to OdhA, the putative E1 subunit of the α-ketoglutarate dehydrogenase complex, and inhibits the activity of the complex. PknG relieves the inhibition by phosphorylation of OdhI.

The function of the mycobacterial homologue of OdhI has not yet been defined, although the gene was named *garA* (glycogen accumulation regulator) for its effects on glycogen metabolism in *Mycobacterium smegmatis* (Belanger and Hatfull, 1999), and the protein was identified as a substrate of PknB in whole-cell protein extracts of *M. tuberculosis* (Villarino *et al*., 2005). GarA consists of a Forkhead-associated (FHA) domain with an N-terminal extension containing the conserved motif ETTS. The phosphorylation site for PknB lies within this motif, while protein–protein interaction is mediated by the FHA domain of GarA and phosphothreonines within the activation loop of PknB (Villarino *et al*., 2005).

Given the high homology between PknG homologues from *C. glutamicum* and *M. tuberculosis*, it seemed likely PknG might regulate metabolism in *M. tuberculosis* by a similar mechanism to that described in *C. glutamicum*. The kinases from the respective organisms (Rv0410c and cg4036) share 45% amino acid identity, whereas GarA (Rv1827) and OdhI share 82%. OdhA shares 59% identity with Rv1248c, but the proteins have been annotated different functions. OdhA is thought to function as the E1 subunit of the α-ketoglutarate dehydrogenase complex in *C. glutamicum* (Niebisch *et al*., 2006). In contrast, *M. tuberculosis* is thought to lack a ketoglutarate dehydrogenase complex, and Rv1248c functions as an α-ketoglutarate decarboxylase (KGD) in a variant tricarboxylic acid cycle (Tian *et al*., 2005).

We sought to characterize the activity of *M. tuberculosis* PknG and investigate whether conservation of function between corynebacteria and mycobacteria could explain the defect in glutamate metabolism observed in mycobacteria lacking PknG (Cowley *et al*., 2004). We show that GarA is a substrate of PknG *in vitro*, and that the high-affinity interaction between the two proteins is mediated through specific binding of GarA to phosphoresidue(s) in the N-terminus of PknG. This protein–protein interaction is recapitulated in living cells of *M. smegmatis*. PknG phosphorylates GarA at T21, which is equivalent to the site of OdhI phosphorylation (Niebisch *et al*., 2006), and adjacent to the residue specifically phosphorylated by PknB (T22) (Villarino *et al*., 2005). Moreover phosphorylation at these two threonines is mutually exclusive *in vitro*, pointing to GarA as a putative phosphorylated intermediate in more than one signalling pathway. The function of GarA in metabolic regulation is investigated, and GarA is found to bind to and modulate the activities of KGD and Rv2476c, the only predicted glutamate dehydrogenase (GDH) encoded in the genome of *M. tuberculosis*.

## Results

### *Autophosphorylation of PknG*

Activation loop phosphorylation is a common mechanism of eukaryotic S/T and tyrosine kinase activation. In *M. tuberculosis*, several receptor-like (*trans*-membrane) S/T protein kinases have been found to display multiple autophosphorylation sites in their activation loop (Boitel *et al*., 2003; Young *et al*., 2003; Durán *et al*., 2005). Phosphorylation of these residues has been shown to modulate kinase activity (Boitel *et al*., 2003; Greenstein *et al*., 2007; Canova *et al*., 2008), much as in their eukaryotic counterparts. We wished to characterize the autophosphorylation of PknG, since this protein lacks a phosphorylation motif in the activation loop, and appears to have no phosphorylated residues in its catalytic domain (Scherr *et al*., 2007). PknG is one of only two soluble S/T protein kinases in *M. tuberculosis*. In addition to the kinase domain, there are N-terminal and C-terminal domains (Fig. 1A). The N-terminal domain contains four cysteines characteristic of the rubredoxin iron-binding motif. Rubredoxins can participate in electron transfer, raising the possibility that PknG activity might be influenced by the redox environment via this domain (Scherr *et al*., 2007). The C-terminus contains a tetratrico-peptide repeat motif (TPR) responsible for dimerization in the crystal structure (Scherr *et al*., 2007).

Recombinant PknG purified from *Escherichia coli* was produced as a phosphoprotein, presumably due to autophosphorylation. To map phosphorylation sites, tryptic peptides were prepared from PknG and the masses compared with a tryptic digest of PstP-treated PknG by MALDI-TOF (PstP is the only S/T phosphatase of *M. tuberculosis*). The N-terminal sequence of PknG (residues 10–60) was systematically detected as unphosphorylated, mono- and diphosphorylated ions, with the relative amount of each species differing between preparations (Fig. 1B). Incubation of PknG with ATP resulted in the disappearance of the unphosphorylated and monophosphorylated ions, confirming that N-terminal phosphorylation was the consequence of an autocatalytic activity (Fig. 1C), whereas phosphate groups were fully removed by PstP (Fig. 1D). Resolution of the sites of phosphorylation was challenging due to the large size of the peptide, but HPLC separation allowed us to recover small amounts of shorter phosphopeptides generated by aberrant trypsin cleavage within the sequence 10–60. Tandem mass spectrometry (MS/MS) experiments on these peptides led to

 

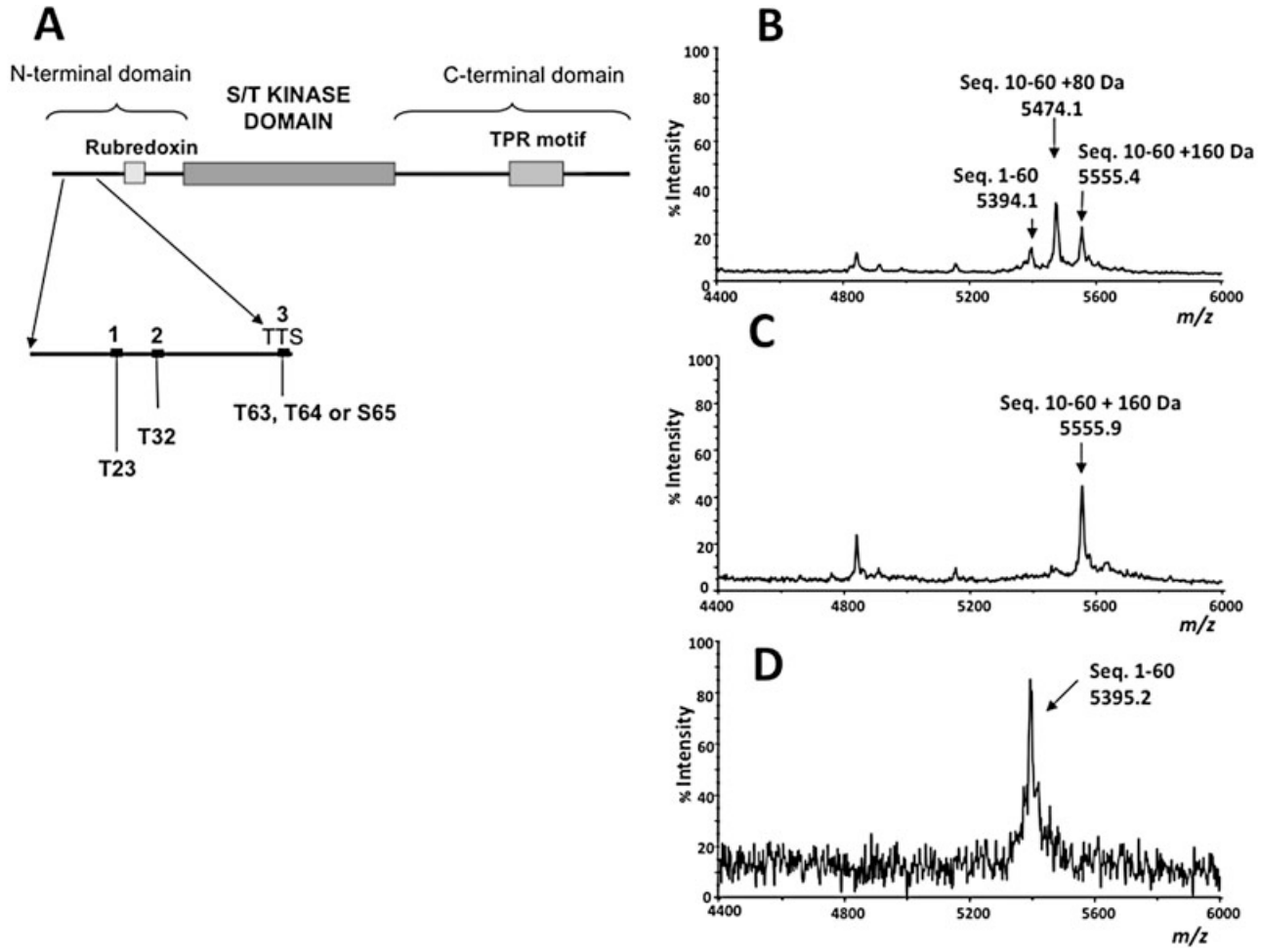


**Fig. 1.** PknG domains and phosphorylation sites.
A. Structure of PknG showing the N-terminal domain containing the rubredoxin motif, the conserved S/T kinase domain and the C-terminal region including the TPR motif (Scherr *et al*., 2007). A cluster of three short sequences containing the autophosphorylation sites in the N-terminal region is shown in the expanded area.
B. Linear MALDI-TOF spectrum of recombinant PknG tryptic digestion. Unphosphorylated, monophosphorylated and diphosphorylated species are indicated by arrows.
C. Linear MALDI-TOF spectrum of peptides generated by tryptic digestion of PknG previously incubated with ATP and $Mn^{2+}$. Diphosphorylated peptide 10–60 is indicated by an arrow.
D. Linear MALDI-TOF spectrum of tryptic digestion of PstP-treated PknG, where the fully dephosphorylated peptide is indicated.

the identification of T23 and either S31 or T32 as the modification sites (Table 1). Additionally, two phosphopeptides were detected by using partial trypsin digestion to increase the sequence coverage to 95% (96% of S and T residues). These were assigned by post-source decay (PSD) fragmentation experiments to mono- and diphosphorylated forms of the peptide sequence 61–73 (*m/z* 1607.5 and *m/z* 1687.6 respectively).

A summary of phosphopeptides and phosphorylated residues identified in this study is shown in Table 1. The N-terminal region of PknG is autophosphorylated, with up to four phosphate groups incorporated into T or S residues. The three motifs containing phosphorylation sites were identified as T23, ST (31–32) and TTS (63–65). The presence of phosphopeptides in each region was confirmed using alternative endopeptidases in place of trypsin.

As a further confirmation of the identification of phosphorylation clusters, putative phosphoresidues were mutated to alanine. Thus, we produced the single mutant T23A, the double mutant S31A/T32A and the triple mutant T63A/T64A/S65A, as well as a truncated form of PknG starting at residue 74 (PknG$\Delta_{1-73}$), which lacks all the detected phosphorylation sites and corresponds to the protein that was structurally characterized by X-ray crystallography (Scherr *et al*., 2007). Peptide mass measurements of tryptic digests from the mutants complemented with binding studies of their interactions with GarA indi-

 

**Table 1.** Identification of phosphopeptides within the N-terminal sequence of PknG.

| Residue | Sequence | $MH^+$ Average theoretical | $MH^+$ Average measured | Number of phosphate groups | Phosphoresidue(s) |
|---|---|---|---|---|---|
| 10–60 | SGPGTQPADAQTATSATVRPLSTQAVFRPDFG DEDNFPHPTLGPDTEPQDR | 5395.7 | 5395.2<br>5475.3<br>5555.4 | 0<br>1<br>2 | Location not identified |
| 29–60 | PLS**T**QAVFRPDFGDEDNFPHPTLGPDTEPQDR | 3597.8 | 3597.5<br>3677.6 | 0<br>1 | T32 |
| 10–30 | SGPGTQPADAQTA**T**SATVRPL | 2027.2 | 2027.3<br>2107.3 | 0<br>1 | T23 |
| 10–28 | SGPGTQPADAQTA**T**SATVR | 1816.9 | 1885.8 | 1 | T23 |
| 61–73 | MA**TTS**RVRPPVRR | 1527.8 | 1607.5<br>1687.6 | 1<br>2 | T63 and/or T64 and/or S65 |

cate that T23 and T32 are phosphorylated in the native protein (data not shown). As expected, the truncated-form PknG$\Delta_{1-73}$ failed to incorporate radiolabelled ATP (data not shown), confirming that all autophosphorylation sites of PknG lie within the N-terminal 73 amino acids. This result is consistent with the reported crystal structure of PknG$\Delta_{1-73}$ in which no phosphogroup has been identified (Scherr *et al*., 2007).

### M. tuberculosis *PknG phosphorylates GarA*

Corynebacterial PknG phosphorylates OdhI at a single threonine residue (T14, corresponding to T21 of GarA) in the motif ETTS (Niebisch *et al*., 2006). In previous work, we have shown that PknB phosphorylates GarA at a single threonine (T22) in the same motif (Villarino *et al*., 2005). To assess the ability of *M. tuberculosis* PknG to phosphorylate GarA, recombinant GarA was incubated with PknG in the presence of ATP and $Mn^{2+}$. Mass analysis revealed an increase of 80 Da in the molecular mass of the whole GarA protein (Fig. 2A and B) and EndoGluC digestion of this protein identified a phosphopeptide (average *m/z* 1453.39, Fig. 2B, inset) corresponding to an increase of 80 Da in sequence 21–32 (average *m/z* 1373.51, Fig. 2A, insert). MS/MS analysis identified the phosphorylated residue as T21, in accordance with the data reported for *C. glutamicum* PknG. Site-directed mutagenesis of GarA confirmed that T21 is the only site of phosphorylation by PknG (Fig. 2E), whereas T22 is the only site of phosphorylation by PknB (Fig. 2F and Villarino *et al*., 2005). Phosphorylation was measured by the incorporation of radiolabel from ATP, and phosphorylated GarA displayed reduced mobility in SDS-PAGE as previously observed for PknB-treated GarA (Villarino *et al*., 2005). The mutant GarA T22A was a substrate for phosphorylation by PknG but the mutant GarA T21A was not (Fig. 2E).

Mass analysis was carried out on GarA phosphorylated using PknB (Fig. 2C), or an equimolar mixture of PknB and PknG (Fig. 2D). In all cases, only mass signals corresponding to monophosphorylated GarA were observed. Incubation with both kinases simultaneously resulted in a mixture of monophosphorylated peptides modified at either T21 or T22, and sequential incubation with each kinase also resulted in only monophosphorylated species, demonstrating that the two phosphorylation events are mutually exclusive *in vitro*.

### *Influence of PknG autophosphorylation on binding to GarA and kinase activity*

To investigate the possible effect of autophosphorylation on PknG activity, we evaluated the ability of both full-length PknG and PknG$\Delta_{1-73}$ to phosphorylate a synthetic peptide corresponding to the GarA sequence 14–30 (SDEVTVETTSVFRADFL), which includes the phosphorylation motif. Both forms of PknG were found to phosphorylate the peptide substrate at T21 with comparable efficiency (Figs S1 and S2). Thus, in contrast to the *trans*-membrane kinases that require autophosphorylation within the activation loop for kinase activity, PknG autophosphorylation does not seem to play a primary activating role. This observation is in agreement with previous data showing that PknG$\Delta_{1-73}$ is able to phosphorylate the full-length kinase-dead mutant (Scherr *et al*., 2007).

Although N-terminal phosphorylation is not essential for kinase activity towards the peptide substrate, when PknG and PknG$\Delta_{1-73}$ were compared using recombinant GarA, the activity of PknG$\Delta_{1-73}$ was fivefold lower than that of the full-length kinase (Fig. S2), while a higher enzyme : substrate ratio was necessary to detect phosphorylation of GarA protein by mass spectrometry (MS) (data not shown), suggesting that the N-terminal phosphoresidues of PknG could play a role in recruitment of GarA via its FHA domain. This hypothesis was tested by *in vitro* interaction studies of PknG with GarA using surface plasmon

 

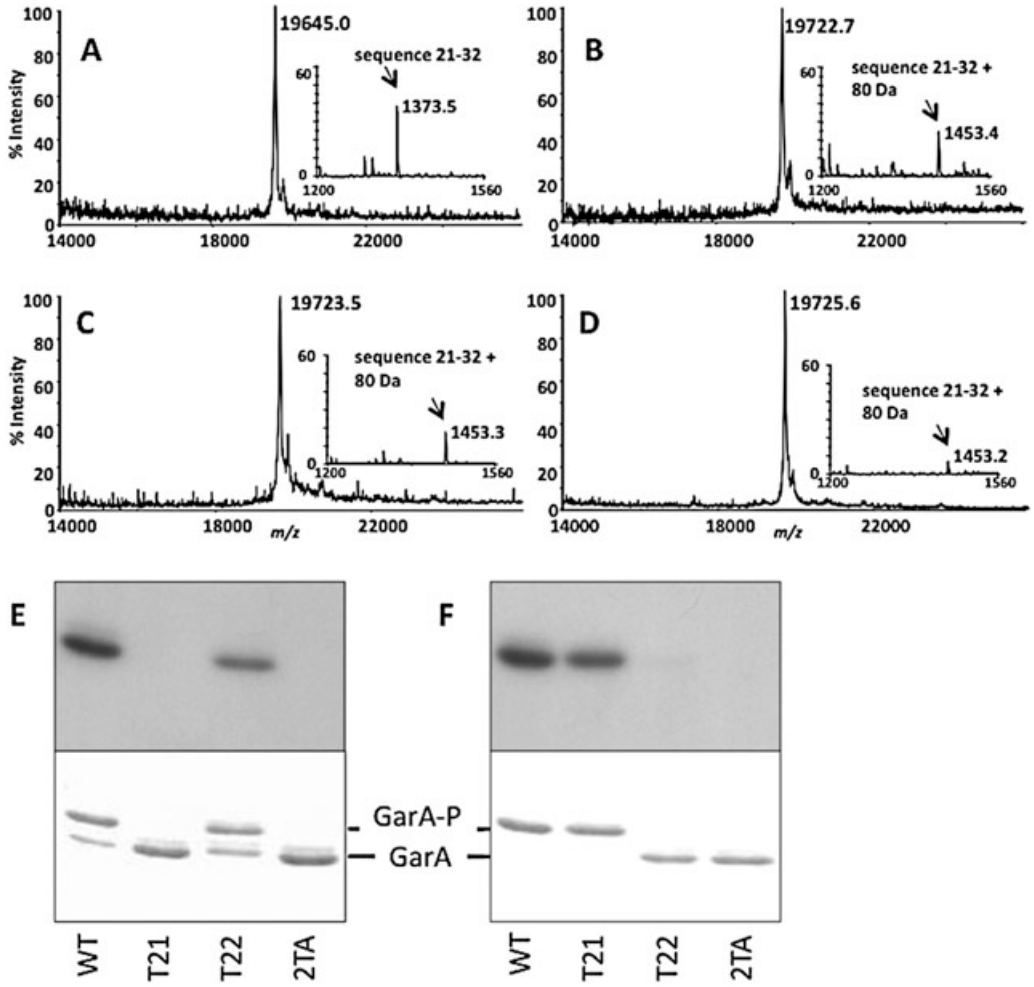


**Fig. 2.** Phosphorylation of GarA by PknG and PknB.
A. Mass spectrum of recombinant GarA. Inset: mass spectrum of EndoGluC digestion of GarA showing the presence of native sequence 21–32.
B. Mass spectrum of GarA phosphorylated by PknG. Inset: mass spectrum of EndoGluC digestion of GarA phosphorylated by PknG showing the presence of phosphorylated sequence 21–32.
C. Mass spectrum of GarA phosphorylated by PknB. Inset: mass spectrum of EndoGluC digestion of GarA phosphorylated by PknB showing the presence of phosphorylated sequence 21–32.
D. Mass spectrum of recombinant GarA phosphorylated by an equimolar mixture of PknG and PknB. Inset: mass spectrum of EndogluC digestion showing the presence of monophosphorylated sequence 21–32.
E. PknG phosphorylates GarA at threonine 21. PknG was incubated with GarA or its mutants in the presence of [$\gamma$-$^{32}$P]-ATP. The identity of the GarA mutant is noted under the lanes; wild type is labelled 'WT' and the double mutant T21A T22A is labelled 2TA. Phosphorylation was detected via the incorporation of $^{32}$P (autoradiogram – top), and by the reduction in mobility of phosphorylated GarA (GarA-P) in SDS-PAGE (Coomassie-stained gel – bottom).
F. PknB phosphorylates GarA at threonine 22. Phosphorylation was assayed as for PknG.

resonance (SPR) biosensor technology. Phosphorylated PknG formed a high-affinity, stable complex with immobilized GarA (Fig. 3A), whereas this interaction was not observed when the kinase was first dephosphorylated (Fig. 3B). Moreover, the synthetic GarA-derived peptide failed to interact with immobilized PknG (at peptide concentrations of 0.50 mM) (data not shown). Furthermore, a stable complex of PknG with GarA was only detected in the absence of ATP. When SPR measurements were attempted in the presence of ATP, the immobilized GarA became phosphorylated and was no longer able to bind PknG (Fig. 3C). These results clearly point to a specific interaction mediated by the GarA FHA domain, as was shown previously for the PknB–GarA complex (Villarino *et al.*, 2005).

### *PknG interacts with GarA in* M. smegmatis

Having established *in vitro* that GarA is a tight-binding substrate of PknG, we wished to confirm the relevance

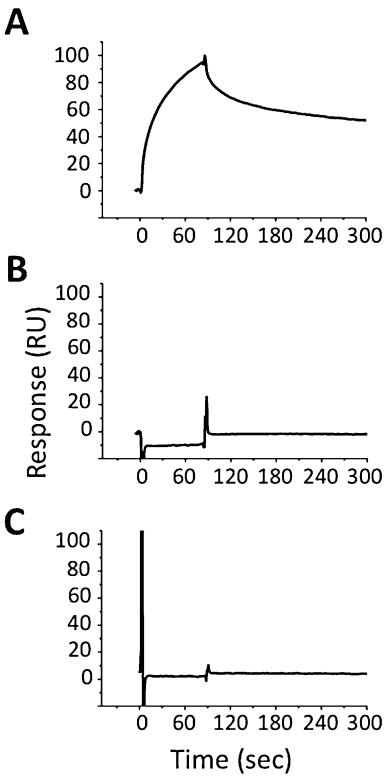


**Fig. 3.** SPR analysis of the interaction between PknG and GarA. GarA was immobilized on a CM5 sensorchip and PknG was injected at time zero for 90 s.
A. Autophosphorylated PknG interacts with GarA.
B. Dephosphorylated (PstP-treated) PknG does not interact with GarA.
C. On-chip phosphorylation of GarA with PknG abolishes the interaction between PknG and GarA.

of this interaction in living mycobacteria using the Split-Trp method to detect protein–protein interaction in non-pathogenic *M. smegmatis* (Tafelmeyer *et al.*, 2004; O'Hare *et al.*, 2008). In this assay, protein interaction leads to reassembly of the fragments of N-(5′-phosphoribosyl)-anthranilate isomerase ($N_{trp}$ and $C_{trp}$) to complement tryptophan auxotrophy. Strains coexpressing $N_{trp}$-PknG with GarA-$C_{trp}$ grew on media lacking tryptophan, suggesting that PknG interacts with GarA in living cells (Fig. S3). $N_{trp}$-PknG was also tested with mutants of GarA-$C_{trp}$, and significantly higher growth rates were observed with GarA mutants that lack the phosphorylation site for PknG (T21), suggesting that only the non-phosphorylated form of GarA can interact with PknG, in agreement with SPR measurements (Fig. 3). Serine S95, which is conserved in the FHA domain family and important for phosphothreonine binding (Durocher *et al.*, 2000), was also mutated, and growth was apparently diminished compared with unmutated GarA, a further indication that the interaction of PknG and GarA is mediated by the FHA domain.

### *GarA is phosphorylated at T21 in mycobacteria grown* in vitro

GarA might be present as a mixture of phosphorylated and unphosphorylated forms in cells, as seen for OdhI (Schultz *et al.*, 2007), and the level of phosphorylation might be controlled by more than one kinase. The phosphorylation status of GarA in cells was investigated directly by purification of phosphopeptides from extracts of *M. tuberculosis* and *M. smegmatis*. In both cases peptides from GarA were among the most abundant phosphopeptides detected. The site of phosphorylation was unambiguously identified as T21 by PSD (Fig. S4). This result does not rule out the presence of GarA phosphorylated at T22 in the cells, but the concentration of any such protein was below the level of detection (more than 10-fold lower than the concentration of GarA phosphorylated at T21). Of the 11 S/T protein kinases of *M. tuberculosis*, four are known to phosphorylate GarA *in vitro* at T22 (PknB, D, E and F) (Villarino *et al.*, 2005) (R. Durán, unpubl. data) but PknG is the only kinase known to phosphorylate T21. Together with the results of *pknG* deletion (Cowley *et al.*, 2004), this observation suggests a direct role for PknG in regulation of GarA-mediated cellular activities.

### *Overexpression of GarA in* M. smegmatis *causes a nutrient-dependent growth defect, which is accentuated by mutation of the phosphorylation sites*

While preparing for the Split-Trp assay we noticed that the transformation efficiency of plasmids encoding $N_{trp}$-GarA was one to two orders of magnitude lower than control plasmids, and the resulting colonies were smaller. The Split-Trp assay was therefore performed using plasmids encoding GarA-$C_{trp}$, which is expressed at a lower level and does not cause an observable phenotype, while the $N_{trp}$-GarA constructs were used to further investigate the effects of overexpression of GarA. The degree of the growth defect was enhanced by point mutations that render GarA non-phosphorylatable. In agreement with the detection of GarA peptides phosphorylated at T21 in mycobacteria, overexpression of the mutant T21A (not phosphorylatable by PknG) gave a stronger phenotype than wild-type GarA, whereas the double mutant 2TA gave no transformants at all (Fig. 4A). The phenotype was dependent on the growth medium and was partly alleviated by supplementation with glutamate, succinate or α-ketoglutarate (Fig. 4B), suggesting a role for GarA and PknG in metabolic regulation. Nevertheless, the additive effect of mutating residues T21 and T22 (Fig. 4A) and the observation that GarA is phosphorylated by different mycobacterial kinases *in vitro* (Durán *et al.*, 2005) might suggest the involvement of other kinases in GarA

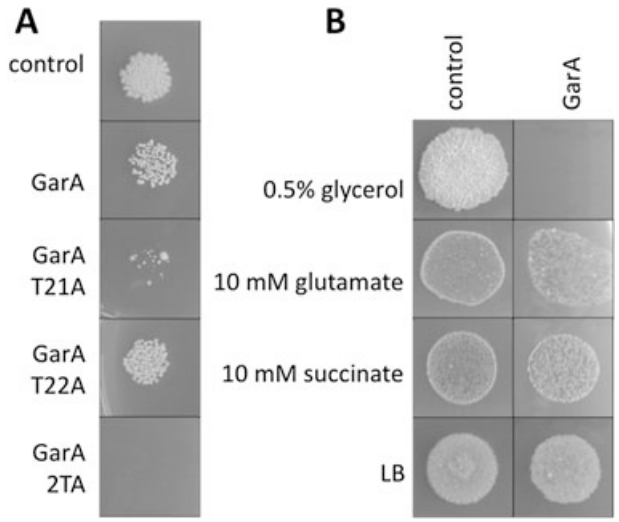


**Fig. 4.** Overexpression of GarA causes a nutrient-dependent growth defect in *M. smegmatis*.
A. The phenotype caused by overexpression of GarA is due to the unphosphorylated form of GarA. *M. smegmatis* transformed with plasmid PL240 'control' or PL240-GarA 'GarA' or mutants of PL240-GarA were spotted onto LB plates.
B. The phenotype caused by overexpression of GarA is nutrient-dependent. *M. smegmatis* transformed with plasmid PL240 'control' or PL240-GarA 'GarA' were spotted onto LB or modified 7H9 lacking glutamate and containing a single carbon source (indicated).

regulation. Since unphosphorylated GarA can form a stable complex with PknG or PknB, it is also possible that overexpression of non-phosphorylatable mutants of GarA may compromise the function of these kinases, which might contribute to the observed phenotype.

### *GarA binds to KGD and GDH*

In order to uncover the molecular basis for the observed effects of GarA on metabolism we used immobilized recombinant GarA to capture potential binding partners from soluble cell extracts of *M. smegmatis* and *M. tuberculosis* (Fig. 5A). Two proteins of approximately 170 and 130 kDa consistently eluted with GarA, but were not captured by Ni-NTA alone. The larger protein was identified as GDH (Rv2476c and MSMEG_4699) by MS and the smaller protein was KGD (Rv1248c and MSMEG_5049) (Table 2). Closer examination of the eluted proteins revealed additional bands of lower intensity, but only one protein was common to samples from both organisms: PknG (Rv0410c and MSMEG_0786) (Table 2).

To clarify the role of phosphorylation we repeated the affinity purification using GarA phosphorylated by PknB or PknG. Neither phosphorylated form of GarA captured any binding partners (Fig. 5B). To test whether binding occurs via the FHA domain, we also tested the mutant S95A, which failed to capture any binding partners. Thus GarA binds to KGD and GDH via the FHA domain, and binding is prevented by phosphorylation at either T21 or T22.

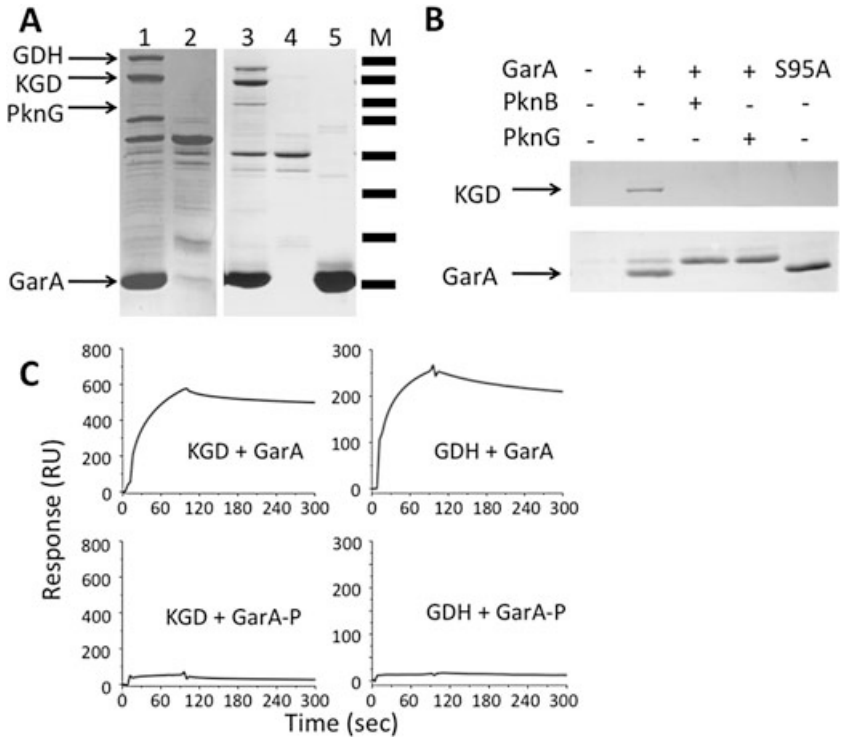


**Fig. 5.** Interaction of unphosphorylated GarA with glutamate dehydrogenase and α-ketoglutarate decarboxylase.
A. Recombinant GarA was used to capture binding partners from cell-free extract of *M. smegmatis* (lane 1) and *M. tuberculosis* (3). Control columns were charged with cell-free extracts but no GarA (2 and 4). Lane 5 contains a sample of the recombinant GarA used in these experiments. M: molecular weight markers of sizes 170, 130, 95, 72, 50, 43, 34, 26 kDa.
B. Recombinant GarA, or the mutant S95A, was phosphorylated by PknB, PknG or neither, and used to capture binding partners from *M. smegmatis* lysate.
C. SPR analysis of the interactions of KGD and GDH with GarA. GarA was immobilized on a CM5 sensorchip and KGD or GDH was injected at time zero for 90 s. On-chip phosphorylation of GarA with PknG prevents any detectable interaction with KGD or GDH.

**Table 2.** Identification of binding partners of GarA by peptide fingerprinting.

| Protein | Gene | MW | Peptides | Coverage (%) | Score |
|---|---|---|---|---|---|
| GDH | Rv2476c | 177 190 | 55 | 60 | 3833 Mascot |
| KGD | Rv1248c | 133 971 | 40 | 59 | 2513 Mascot |
| PknG | Rv0410c | 81 577 | 15 | 22 | 599 Mascot |
| GDH | MSMEG_4699 | 173 965 | 42 | 39 | 408.0 Phenyx |
| KGD | MSMEG_5049 | 135 813 | 31 | 40 | 291.5 Phenyx |
| PknG | MSMEG_0786 | 82 644 | 19 | 39 | 177.0 Phenyx |

MW, molecular weight.

These findings were confirmed using SPR to measure the interaction of GarA with recombinant KGD and GDH: complex formation was observed with immobilized GarA, but not with GarA phosphorylated by PknG (Fig. 5C).

### *GarA inhibits the activity of KGD*

Having identified GarA as a binding partner of two enzymes involved in pathways of glutamate metabolism, KGD and GDH, we next investigated whether binding to GarA has a direct influence on these two enzyme activities. Each activity was assayed using both native proteins and then using purified recombinant proteins.

The activity of KGD was measured in cell-free extracts of *M. smegmatis* using the ferricyanide reductase assay (Tian *et al.*, 2005). Ferricyanide reduction was measured as 20 nmol $min^{-1}$ $mg^{-1}$ protein and was dependent on α-ketoglutarate and thiamine pyrophosphate (TPP). This activity was reduced by a factor of three (7 nmol $min^{-1}$ $mg^{-1}$) upon addition of GarA (1 μM), but was unaffected by addition of an equal concentration of phosphorylated GarA.

Recombinant KGD (MSMEG_5049) was purified from *E. coli* and showed maximal ferricyanide reductase activity of 1.6 $s^{-1}$ or 690 nmol $min^{-1}$ $mg^{-1}$ and $K_m$ for α-ketoglutarate of 540 μM (Fig. 6A), similar to the *M. tuberculosis* homologue Rv1248c (1.8 $s^{-1}$ and 480 μM) (Tian *et al.*, 2005). Addition of recombinant GarA, but not phosphorylated GarA, resulted in concentration-dependent inhibition of the ferricyanide reductase activity (Fig. 6B). The affinity of KGD for GarA must be high since the concentration of GarA that gave half-maximal inhibition (53 nM) was close to the concentration of KGD in the assay (57 nM). At the highest concentration of GarA, KGD activity was sevenfold lower than that of the uninhibited reaction (Fig. 6B). Inhibition was apparently non-competitive for α-ketoglutarate (Fig. 6A).

### *GarA inhibits the activity of GDH*

Assay of GDH activity in cell lysates of *M. smegmatis* was prevented by the presence in the genome of three predicted GDHs, but native MSMEG_4699 could be partially purified via its affinity for GarA (purified as shown in Fig. 5A). The activity was measured by the consumption of NADH in the presence of α-ketoglutarate and ammonium chloride. The GDH activity of this protein mixture was low, 18 nmol $min^{-1}$ $mg^{-1}$, but activity increased to 88 nmol $min^{-1}$ $mg^{-1}$ upon phosphorylation of GarA by PknB. Subsequent addition of unphosphorylated GarA (2 μM) reduced the activity to 15 nmol $min^{-1}$ $mg^{-1}$.

MSMEG_4699 shares 68% amino acid identity with Rv2476c, the sole predicted GDH of *M. tuberculosis*. These previously uncharacterized proteins belong to the family of GDH-4 proteins, which are large tetrameric enzymes specific for $NAD^+$ (Minambres *et al.*, 2000; Lu and Abdelal, 2001; Andersson and Roger, 2003; Kawakami *et al.*, 2007). In order to investigate the mode of inhibition of GDH by GarA, MSMEG_4699 was expressed and purified from *E. coli*. Activity was optimal at pH 8.5, and was stimulated by addition of manganese and magnesium. MSMEG_4699 is highly specific for $NAD^+$,

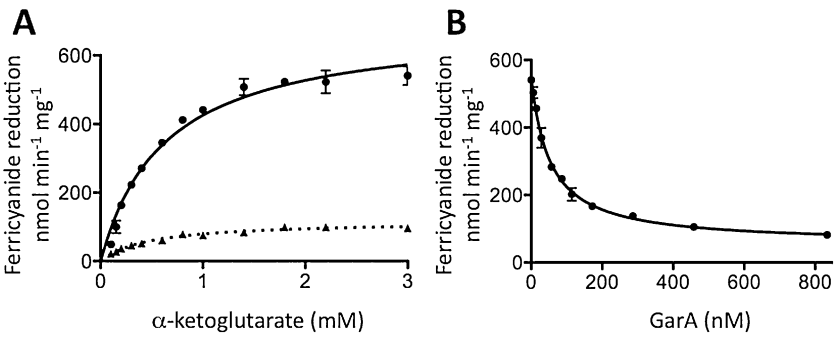


**Fig. 6.** Inhibition of KGD by GarA
A. Ferricyanide reductase activity of KGD was measured at various α-ketoglutarate concentrations, in the presence of 2 μM GarA (triangles, dashed line) or without GarA (circles, solid line).
B. Concentration-dependent inhibition of KGD by GarA, measured at 3 mM α-ketoglutarate.

 

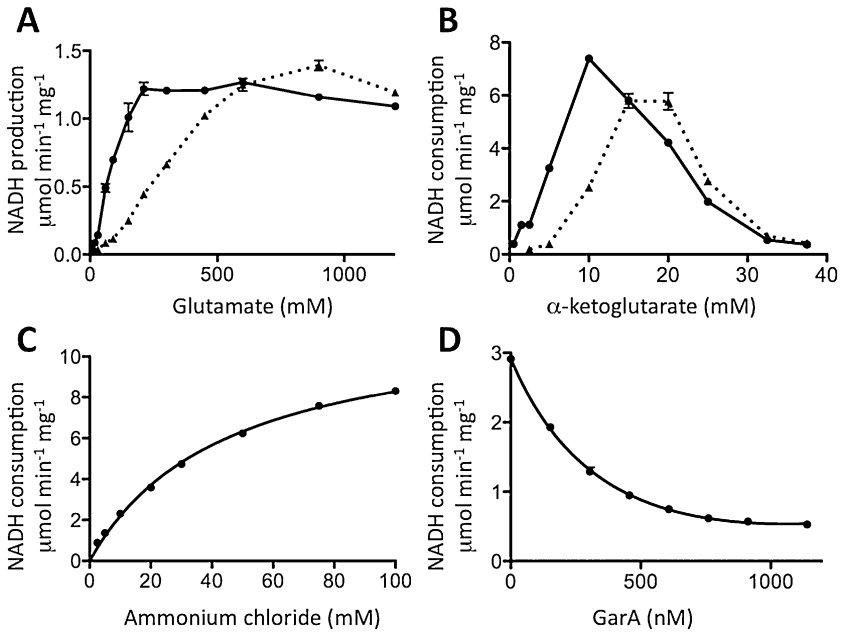


**Fig. 7.** Characterization of GDH and its regulation by GarA.
A. The oxidative deamination activity of GDH was measured at various concentrations of glutamate, in the presence of 2 µM GarA (triangles, dashed line) or without GarA (circles, solid line).
B. The reductive amination activity of GDH was measured at various α-ketoglutarate concentrations with 50 mM ammonium chloride and 2 µM GarA (triangles, dashed line) or without GarA (circles, solid line).
C. The ammonium dependence of reductive amination was measured at 4 mM α-ketoglutarate.
D. Concentration-dependent inhibition of GDH reductive amination activity by GarA was measured at 3 mM α-ketoglutarate and 50 mM ammonium chloride.

and no reaction could be detected using 5 mM $NADP^+$. The glutamate binding curve was sigmoidal, with maximal activity of 3.7 $s^{-1}$ (1.3 µmol $min^{-1}$ $mg^{-1}$) and half-maximal activity observed at 83 mM glutamate (Fig. 7A). Addition of GarA, but not phosphorylated GarA, led to a change in the affinity for glutamate so that maximal activity was observed at 300 mM glutamate (Fig. 7A). At lower glutamate concentrations (below 600 mM) GarA inhibited GDH activity up to sixfold, but when the glutamate concentration exceeded 600 mM the addition of GarA caused a small increase in GDH activity.

The reaction catalysed by GDH is reversible, and reductive amination of α-ketoglutarate was also studied. Severe substrate inhibition was observed above 10 mM α-ketoglutarate (Fig. 7B). The maximum rate of 24 $s^{-1}$ (8.3 µmol $min^{-1}$ $mg^{-1}$) was measured at 10 mM α-ketoglutarate and the $K_m$ of GDH (MSMEG_4699) for ammonium was calculated as 45 mM at 4 mM α-ketoglutarate (Fig. 7C). As shown in Fig. 7B, addition of GarA reduced the maximal rate of amination by GDH (MSMEG_4699), and changed the affinity for α-ketoglutarate such that the maximal rate was observed at 17.5 mM α-ketoglutarate. At saturating GarA concentrations the reaction was inhibited 5.5-fold, and half-maximal inhibition was seen at 540 nM GarA.

## Discussion

The prevalence of S/T protein kinases in the genome suggests that S/T phosphorylation is an important means of signal transduction in *M. tuberculosis* and this has been borne out by the identification of roles for S/T phosphorylation in regulation of enzyme activity, regulation of transcription and control of nutrient transport (reviewed by Wehenkel *et al.*, 2008). While differential gene expression is an important response to changing environmental stimuli, post-translational mechanisms also regulate protein functions and enzyme activities in prokaryotes (Mascher *et al.*, 2006). Regulation of enzyme activity may occur by direct phosphorylation, as in the well-studied example of isocitrate dehydrogenase of *E. coli* (Garnak and Reeves, 1979). More recently, PknG of *C. glutamicum* was shown to act indirectly to regulate the activity of the α-ketoglutarate dehydrogenase complex by phosphorylation of the regulatory protein OdhI (Niebisch *et al.*, 2006). This mechanism of indirect post-translation regulation via a phosphoprotein is unusual, but would potentially allow the co-ordinated regulation of more than one enzyme activity.

Apart from regulation of cellular functions, secreted S/T protein kinases of bacterial pathogens may function as virulence factors (Cozzone, 2005). In *M. tuberculosis*, PknG is thought the most likely kinase to be directly involved in pathogenesis since strains lacking *pknG* have attenuated virulence in a mouse model and reduced survival inside macrophages, although no molecular mechanism is known (Walburger *et al.*, 2004). In addition to the attenuation of virulence, *pknG* deletion mutants of *M. tuberculosis* (Cowley *et al.*, 2004), but not *Mycobacterium bovis* BCG (Nguyen *et al.*, 2005), showed evidence of a defect in metabolism, raising the question that metabolic perturbations might be responsible for the reduced virulence of the *pknG* deletion strain. Together with the homology to the equivalent kinase of *C. glutamicum*

 

(Niebisch *et al*., 2006), this prompted our investigation into the autophosphorylation, substrate specificity and function of PknG.

*Corynebacterium glutamicum* PknG is devoid of autophosphorylation activity, and must first be phosphorylated in the C-terminal domain by PknA in order to become active towards its substrate OdhI (Fiuza *et al*., 2008). PknA phosphorylates PknG at residues T451 and T787, which may aid substrate recruitment by interaction with the FHA domain of OdhI. Sequence comparison shows that neither threonine is conserved in *M. tuberculosis* PknG; in fact, MS and mutagenesis revealed that the pattern of phosphorylation and the mechanism of activation are very different from the corynebacterial homologue and also from any of the transmembrane S/T protein kinases of *M. tuberculosis* previously characterized (Fig. 1, Table 1). We found that PknG shows autokinase activity, incorporating up to four phosphate groups in the N-terminus: T23 and T32 plus two sites within the sequence T63/T64/S65. No phosphorylation sites were found in the activation loop or in the C-terminal TPR domain. This is in agreement with the lack of autokinase activity of the N-terminally truncated form of PknG (which nevertheless shows transphosphorylation activity) and the absence of phosphorylation sites in the crystal structure of this protein (Scherr *et al*., 2007).

Although the phosphorylation pattern and mechanism of activation differ between PknG homologues in *M. tuberculosis* and *C. glutamicum*, they share a common substrate, GarA or OdhI, and each phosphorylates the first threonine of the conserved motif ETTS (T21 of GarA). This is in contrast to PknB and other *M. tuberculosis* S/T protein kinases that phosphorylate the second threonine (T22). Using a peptide substrate we found that the specificity of phosphorylation is determined by local structural factors, since the peptide is phosphorylated at the same residue as the full-length protein, but the lower efficiency of peptide phosphorylation suggested that the whole protein substrate is important for efficient kinase–substrate docking. SPR measurements indicate a high affinity interaction between the FHA domain of GarA and phosphothreonine(s) at the N-terminus of PknG. The role of phosphothreonines in substrate recruitment is further supported by the lower activity of PknG$\Delta_{1-73}$ (which lacks all phosphorylation sites) towards GarA. Thus the mechanism of substrate recruitment may be conserved between corynebacterial and mycobacteria, although the phosphothreonines are in different domains.

GarA is the substrate of several S/T protein kinases of *M. tuberculosis*, and substrate promiscuity of kinases is a known phenomenon under *in vitro* conditions; therefore, the *in vitro* assays of PknG binding and phosphorylation of GarA were complemented with other methods to show that PknG and GarA interact with each other *in vivo* (Fig. S3), that GarA is phosphorylated at T21 *in vivo* (Fig. S4) and that residues T21 and T22 are important for the function of GarA in *M. smegmatis* (Fig. 4).

The results of GarA overexpression were indicative of a role for unphosphorylated GarA in metabolic regulation (Fig. 4) and we used affinity purification to uncover the molecular mechanism (Fig. 5A and B). The possible regulation of KGD (Rv1248c) by GarA has been postulated (Bott, 2007) but remained to be established experimentally, given the different predicted functions of OdhA (part of the α-ketoglutarate dehydrogenase complex) and *M. tuberculosis* Rv1248c (KGD). These two proteins share an unusual domain structure that is conserved between corynebacteria, mycobacteria and other actinobacteria, but so far unique to this phylum (Usuda *et al*., 1996; Niebisch *et al*., 2006). The C-terminus of Rv1248c is homologous to the E1 subunit of the α-ketoglutarate dehydrogenase complex, while the N-terminus is homologous to the acyltransferase domain of the E2 subunit of the same complex. As mentioned above, mycobacteria are thought to lack the α-ketoglutarate dehydrogenase complex. KGD and succinic semialdehyde dehydrogenase form an alternative pathway to succinate. It is possible that this unusual TCA cycle is also present in other actinobacteria. Indeed, although OdhA of *C. glutamicum* has so far been thought to function as part of an α-ketoglutarate dehydrogenase complex, the data might also be explained by the coupled activities of KGD and succinic semialdehyde dehydrogenase (Niebisch *et al*., 2006).

GarA was found to inhibit *M. smegmatis* KGD, and it is likely that it also inhibits KGD in *M. tuberculosis*, given the high homology (83% amino acid identity) between MSMEG_5049 and Rv1248c, and the fact that both proteins could be purified by their affinity for GarA (Fig. 5A). It is also possible that this mechanism operates in other actinomycetes, since homologues of GarA and PknG are found in mycobacteria, corynebacterial, rhodococci, nocardia, frankia and streptomyces (Niebisch *et al*., 2006).

The purification of GDH by its affinity to GarA was unexpected, since this enzyme was not found in the study of *C. glutamicum*; indeed, Rv2476c ($NAD^+$-specific GDH-4) shares very little homology with cg2280 ($NADP^+$-specific, family GDH-1) (Bormann *et al*., 1992), limited to a few residues directly involved in substrate binding. Only four members of the GDH-4 family have been characterized previously (Minambres *et al*., 2000; Lu and Abdelal, 2001; Camardella *et al*., 2002; Kawakami *et al*., 2007). Our characterization of MSMEG_4699 revealed similarities to the homologous enzyme from *Streptomyces clavuligerus* in terms of the maximum enzyme activity, $K_m$ for ammonium and affinity for α-ketoglutarate (24 μmol $min^{-1}$ $mg^{-1}$, 45 mM ammo-

nium and half-activity at 5 mM α-ketoglutarate, compared with 21 μmol $min^{-1}$ $mg^{-1}$, 34 mM ammonium and 1.3 mM α-ketoglutarate) (Minambres *et al*., 2000). Two features of MSMEG_4699 are unusual: the severe substrate inhibition by α-ketoglutarate and the low affinity for glutamate. Half-maximal activity was seen at 83 mM glutamate, compared with 4.4 mM for the GDH from *Pseudomonas aeruginosa* and 7.1 mM for the GDH from *Janthinobacterium lividum* (Lu and Abdelal, 2001; Kawakami *et al*., 2007). This low affinity tallies with the high intracellular glutamate concentration of *M. tuberculosis*, which has been estimated as approximately 80 mM, but may be as high as low molar concentrations (Tian *et al*., 2005).

It is not known whether the function of *M. tuberculosis* GDH is predominantly anabolic or catabolic. Both reactions are affected by GarA and in both cases GarA alters the affinity of GDH for the substrate. Whether GarA is an activator or an inhibitor under physiological conditions depends on the substrate concentration. However, assuming that physiological concentrations of α-ketoglutarate are similar to those estimated in *E. coli* (0.1–0.9 mM) *and C. glutamicum* (1 mM) (Senior, 1975; Müller *et al*., 2006) and that intracellular concentration of glutamate is below 600 mM, then GarA would inhibit GDH activity.

α-Ketoglutarate is the substrate of both KGD and GDH, and lies at an important branch point of metabolism since it can either be oxidized in the TCA cycle or be converted to glutamate either by GDH (under conditions of nitrogen abundance) or by the combined actions of glutamine synthetase and glutamate synthase (in nitrogen limitation). KGD and GDH have differing affinities for α-ketoglutarate, with KGD having a $K_m$ of 0.5 mM and GDH showing half-maximal activity at 5 mM. As seen in Figs 6 and 7, GarA is a non-competitive inhibitor of KGD whereas it reduces the affinity of GDH for α-ketoglutarate, thus the unphosphorylated form of GarA could alter the flux of α-ketoglutarate towards glutamate production. This has been studied in more detail in *C. glutamicum*, which is used industrially to produce glutamate. In this organism deletion of *odhI* abolishes glutamate production, whereas deletion of *pknG* increases production under some conditions (Schultz *et al*., 2007). Similarly, deletion of *pknG* causes glutamate accumulation in *M. tuberculosis* (Cowley *et al*., 2004), although not in *M. bovis* BCG (Nguyen *et al*., 2005), presumably due to the extensive metabolic differences between the strains that arose during the attenuation process (Brosch *et al*., 2007). For *C. glutamicum* it has been shown that PknG senses the nutritional status, either directly or indirectly, since OdhI is predominantly phosphorylated in bacteria grown in rich broth but mainly unphosphorylated in bacteria grown in minimal medium (Schultz *et al*., 2007).

The FHA domain of GarA is apparently able to interact not only with phosphoproteins via the recognition of phosphothreonine residues (PknG and PknB; Fig. 3 and Villarino *et al*., 2005) but also with unphosphorylated proteins (Fig. 5C, since recombinant KGD and GDH are unlikely to become phosphorylated during expression in *E. coli*, and preliminary observations). Several observations in this study can be best explained by a model of GarA autorecognition, in which the phosphothreonine at the N-terminus of GarA binds to the FHA domain in an intramolecular reaction (P. England, submitted). This model explains why phosphorylation of T21 and T22 are mutually exclusive events (Fig. 2), and how phosphorylation of GarA acts as a molecular switch to prevent FHA domain-dependent interactions with PknG, KGD and GDH (Figs 3 and 5, Fig. S3). The results presented in Fig. 4 and Fig. S4 suggest that PknG may be involved, possibly with other kinase(s), in the switch between the active (unphosphorylated) and inactive forms of GarA.

The interaction of PknG with GarA is unusually strong for a kinase–substrate complex (Fig. 3), allowing this kinase to be isolated from cell lysates of *M. tuberculosis* and *M. smegmatis* by affinity purification (Fig. 5A and Table 2). The low amount of PknG purified in this way probably reflects a low cellular concentration of PknG (and other S/T protein kinases), which could not be detected in proteomic studies of *M. smegmatis* and *M. tuberculosis* (Pleissner *et al*., 2004; Wang *et al*., 2005). Our results on the purification of *M. smegmatis* PknG are in contradiction with a previous report claiming that *M. smegmatis* lacks this kinase (Walburger *et al*., 2004). Possibly, the failure to detect PknG by immunoblotting assays in that study may be due to both low protein abundance and antibody specificity (the antibody was raised against *M. tuberculosis* PknG, which shares 76% sequence identity with MSMEG_0786). The interpretation of the results by Walburger *et al.* presumed that *M. smegmatis* lacks PknG, hence changes in lysosomal transport caused by ectopic expression of *M. tuberculosis* PknG in *M. smegmatis* were evidence of a direct role of PknG in preventing lysosomal transfer. In contrast, we observed that PknG is expressed in *M. smegmatis* and the native kinase binds to GarA, suggesting a role for PknG in maintaining general mycobacterial physiology in both pathogenic and non-pathogenic strains. Such a role has been postulated previously, based on the ubiquity of PknG homologues in mycobacterial genomes, although differences in the N-termini could be indicative of functional differences (Narayan *et al*., 2007). Thus, while we have not investigated a direct role for PknG as a virulence factor, we have presented evidence for a role of PknG in metabolic regulation via control of the phosphorylation status of GarA. Deficiencies in primary metabolism could

 

contribute to the attenuated virulence of *pknG* deletion strains of *M. tuberculosis*.

## Experimental procedures

### *Cloning and mutagenesis*

Oligonucleotides are listed in Table S1. Plasmid pM20, for expression of PknG (Rv0410c) with a hexahistidine tag (removable using tobacco etch virus protease, TEV), was constructed by PCR of the gene from cosmid MTCY22G10 (S. Cole), digestion and ligation into the EcoRI site of the pET28a vector (Novagen). The correct sequence of all constructs was verified by DNA sequencing. Plasmid PL383 encoding GarA with a hexahistidine tag was constructed by PCR amplification of Rv1827 from genomic DNA of *M. tuberculosis* H37Rv. The gene was digested and cloned into the NdeI/BamHI sites of pET15b (Novagen). Mutants of GarA (Rv1827) were constructed using pairs of complementary primers to encode the desired mutation. Rv1827 was also cloned into the pDEST17 Gateway expression vector (Invitrogen) with a TEV cleavage site for removal of the hexahistidine tag. The genes encoding GDH (MSMEG_4699) and KGD (MSMEG_5049) were amplified from *M. smegmatis* genomic DNA by PCR and ligated into pET28a cut with NheI and EcoRI to produce plasmids PL493 and PL494. Plasmids for the Split-Trp assay were constructed by PCR amplification of PknG, GarA, or mutants of GarA, and ligation of the products into PL240 or PL242 cut with SpeI and HpaI.

### *Protein purification*

PstP (Rv0018c) and PknB (Rv0014c) were purified as described previously (Boitel *et al.*, 2003; Ortiz-Lombardía *et al.*, 2003; Pullen *et al.*, 2004).

### *Purification of untagged PknG and PknG$\Delta_{1-73}$*

Full-length PknG was overexpressed in *E. coli* BL21(DE3) cells grown for 24 h at 30°C without IPTG; the truncated variant PknG$\Delta_{1-73}$ was expressed in the same strain after 16 h induction at 14°C with 1 mM IPTG. Both proteins were then purified following the same protocol. Frozen *E. coli* cell pellets were re-suspended in lysis buffer (25 mM $NaH_2PO_4$, 500 mM NaCl, 5% glycerol, 25 mM imidazole, pH 8.0) supplemented with Complete protease inhibitor cocktail (Roche). The lysate was centrifuged at 26 800 *g* for 1 h, filtered (0.45 µm) and loaded onto a 5 ml HisTrap $Ni^2$ ± IMAC column (GE Healthcare) equilibrated in lysis buffer; the recombinant protein was then purified applying a linear imidazole gradient (20–400 mM). The PknG-containing fractions, as verified by 12% SDS-PAGE, were dialysed overnight at 4°C against 50 mM Tris-HCl pH 8.0, 500 mM NaCl, 5% glycerol, and the $His_6$ tag was removed by incubation for 24 h at 4°C in the presence of $His_6$-tagged TEV protease (van den Berg *et al.*, 2006) at a 1:30 ratio (w/w) followed by separation on Ni-NTA agarose column (Qiagen). The digestion mixture was then passed through 1 ml of Ni-NTA resin (Qiagen) by gravity flow to separate PknG from the cut histidine tag and the protease. The untagged PknG was then further purified by size-exclusion chromatography on a Superdex 200 26/60 column (GE Healthcare) equilibrated in either Tris-HCl pH 8.0, 250 mM NaCl, 5% glycerol (full-length PknG) or Tris-HCl pH 8.0, 500 mM NaCl, 5% glycerol (PknG$\Delta_{1-73}$). Fractions corresponding to the PknG peak, as confirmed by SDS-PAGE, were pooled and concentrated up to 40 mg $ml^{-1}$ with 10 kDa cut-off Vivaspin concentrators (Sartorius). The concentrated protein, with a purity >95% as estimated by Coomassie blue staining after SDS-PAGE, was flash-frozen in liquid nitrogen and stored at –80°C.

### *Purification of hexahistidine-tagged GarA, or mutants of GarA, or MSMEG_3647*

BL21(DE3) carrying plasmid PL383 (or mutants thereof) were grown in LB medium at 37°C until $OD_{600}$ = 0.6, then for 4 h at 27°C after addition of 1 mM IPTG. The cells were harvested by centrifugation and re-suspended in phosphate-buffered saline (PBS) supplemented with PMSF 1 mM. GarA was purified using Ni-NTA agarose, and stored in PBS at 4°C.

### *Purification of untagged GarA*

BL21(DE3)pLysS carrying pDEST17-GarA were grown in HDM2 medium in 70 ml microfermentors, first at 30°C until $OD_{600}$ 20 was reached, then for 16 h at 14°C after addition of 1 mM IPTG (final $OD_{600}$ between 60 and 70). The cells were harvested by centrifugation and re-suspended in buffer B (25 mM HEPES, 500 mM NaCl, 20% glycerol, 1 mM DTT, 20 mM imidazole, pH 8.0) supplemented with Complete protease inhibitor cocktail (Roche). $His_6$-tagged GarA was first purified by metal-affinity chromatography on a nickel-loaded HisTrap HP column (GE Healthcare) equilibrated in buffer B, using a linear imidazole gradient (20–500 mM). The GarA-containing fractions were dialysed against buffer C (25 mM HEPES, 100 mM NaCl, 5% glycerol, 1 mM DTT, pH 8.0), and the $His_6$ tag was removed by incubation for 24 h at 18°C in the presence of $His_6$-tagged TEV endoprotease at a 1:70 ratio followed by separation on Ni-NTA agarose column (Qiagen). The untagged GarA was then further purified by size-exclusion chromatography on a Superdex 75 column (GE Healthcare) equilibrated in buffer B.

### *Purification of KGD (MSMEG_5049)*

BL21(DE3) carrying the appropriate plasmid were grown in LB medium at 37°C until $OD_{600}$ 0.6, then for 16 h at 14°C after addition of 1 mM IPTG. Cells were re-suspended in 50 mM MOPS pH 7.5, 150 NaCl supplemented with 1 mM PMSF. The protein was purified using Ni-NTA agarose, then equilibrated in 50 mM MOPS pH 7.5, 150 NaCl plus 1 mM $MgCl_2$ and stored at 4°C.

### *Purification of GDH (MSMEG_4699)*

BL21(DE3) carrying the appropriate plasmid were grown in LB medium at 37°C until $OD_{600}$ 0.6, then for 16 h at 14°C after addition of 1 mM IPTG. Cells were re-suspended in 50 mM MOPS pH 7.5, 150 mM NaCl supplemented with 1 mM

 

PMSF. The protein was purified using Ni-NTA agarose, then equilibrated in 50 mM MOPS pH 8.0, 1 mM $MgCl_2$ and stored at 4°C.

### *Protein kinase assay*

Protein phosphorylation reactions were performed in 50 mM HEPES buffer pH 7.0 containing 1 mM DTT, 2 mM $MnCl_2$ and 50 μM ATP. Activities of PknG and PknG$\Delta_{1-73}$ were assayed using either recombinant GarA or a synthetic peptide corresponding to GarA sequence 14–30 (SDEVTVETTSVFRADFL). The molar ratio of kinase : substrate ranged from 1:3 to 1:100. Reaction mixtures were incubated at 35°C and substrate phosphorylation was evaluated by MS. In the case of protein substrates, increased sensitivity was achieved by monitoring phosphorylation at specific peptides by MS measurements after EndoGluC digestion. The same experimental procedure was used for testing PknB kinase activity. The autophosphorylation activity of PknG and PknG$\Delta_{1-73}$ was assessed by incubation of the enzymes in the presence of 50 μM ATP for 20 min at 35°C. The samples were then digested with trypsin and phosphopeptides were detected by MS.

### *Radioactive protein kinase assay*

Phosphorylation reactions were performed in 50 mM HEPES buffer pH 7.0 containing 5 mM $MgCl_2$ and 2 mM $MnCl_2$. The concentration of kinase (PknG, PknG$\Delta_{1-73}$ or PknB) was 175 nM and the concentration of GarA (or mutants thereof) was 7.7 μM. Reactions were started by the addition of a mixture of [$\gamma$-$^{32}$P]-ATP and unlabelled ATP to give a final concentration of 100 μM ATP and 50 nCi $\mu l^{-1}$. Reactions were incubated at 37°C for 60 min (Fig. 2) or 5–60 min (Fig. S2) then stopped by the addition of SDS to 1% and analysed by SDS-PAGE with Coomassie staining and autoradiography. The relative amount of phosphorylated GarA was estimated from the autoradiogram using a GS710 densitometer and Quantity One software (Bio-Rad).

### *Protein dephosphorylation*

Dephosphorylation was carried out by incubation of recombinant PknG (5–20 mM) with purified PstP (phosphatase : substrate ratios 1:5 to 1:10) in 50 mM HEPES buffer, pH 7.0, containing 1 mM DTT, 2 mM $MnCl_2$ for 1 h at 35°C. In some experiments, alkaline phosphatase from calf intestine (Roche Diagnostics) was used for enzymatic dephosphorylation.

### *Sample preparation for MS*

Enzymatic digestion was carried out by incubation of recombinant PknG with trypsin (Promega) in 50 mM ammonium bicarbonate pH 8.3 overnight at 35°C (enzyme/substrate ratios 1/10 to 1/50 w/w). Peptides generated by partial tryptic cleavage were obtained by incubation with trypsin (enzyme/substrate ratio 1/1000 w/w), for 10 min at 35°C. Alternatively EndoGluC and EndoAspN were used as proteolytic enzymes. HPLC separations were performed on a reverse-phase column (Vydac C18, 1 × 150 mm) equilibrated with 0.1% trifluoroacetic acid and eluted with 0.07% trifluoroacetic acid in a linear gradient of acetonitrile from 0% to 50% in 100 min. The eluate was monitored at 220 nm and fractions were collected and analysed by MS.

Mass spectrometry measurements were carried out in a Voyager DE-PRO MALDI-TOF (Applied Biosystems) or in a 4800 MALDI TOF-TOF Analyser (Applied Biosystems). The molecular mass of the native and phosphorylated protein substrates was determined using a sinapinic acid matrix (10 mg $ml^{-1}$ in acetonitrile–$H_2O$ 50%, 0.2% trifluoroacetic acid) with cytochrome *c* as an external standard. Mass spectra of digestion mixtures or isolated peptides were acquired on linear and reflector modes using a matrix solution of α-cyano-4-hydroxycinnamic acid in 0.2% trifluoroacetic acid in acetonitrile–$H_2O$ (50%, v/v) and were externally calibrated using a mixture of peptide standards (Applied Biosystems). The presence of phosphopeptides was confirmed by the characteristic fragmentation pattern when analysed by PSD MS, allowing the determination of the number of phosphate groups. Identification of phosphoresidues was performed by MS/MS analysis of HPLC-purified fractions from proteolytic digestions. In some cases in-source decay fragmentation (ISD) or MS/MS analysis of HPLC-purified phosphopeptides allowed the assignment of phosphorylation sites to short peptide sequences

### *Surface plasmon resonance*

Surface plasmon resonance experiments were performed on a BIAcore 3000 instrument (BIAcore, Piscataway, NJ). GarA was immobilized using standard amine-coupling procedures (Amine Coupling Kit, BIAcore) on a CM5 sensorchip at pH 5 to a final density of 550 resonance units (RU) and then the instrument was primed five times with running buffer (HBS-EP: 20 mM HEPES pH 7.4, 150 mM NaCl, 3 mM EDTA, 0.005% P20). A flow cell activated and blocked with ethanolamine was left as a control surface for non-specific binding. Binding experiments were performed at 25°C at a flow rate of 20 $\mu l$ $min^{-1}$ using association and dissociation times of 90 s and 210 s respectively. Thirty microlitres of 200 nM PknG, 1000 nM KGD or 1000 nM GDH were injected onto the surfaces, and afterwards the surface was regenerated by injecting 10 mM NaOH for 18 s at a flow rate of 100 $\mu l$ $min^{-1}$. All data processing was carried out using the BIAevaluation 4.1 software provided by BIAcore.

GarA was phosphorylated on-chip by injecting 150 μl of 1 μM PknG during 30 min at a flow rate of 5 $\mu l$ $min^{-1}$ in kinase buffer (50 mM HEPES buffer pH 7.0 containing 1 mM DTT, 2 mM $MnCl_2$ and 50 μM ATP).

Binding responses were first double-referenced by subtracting signals corresponding to both reference flow cell and from the average of blank (buffer) injections.

### *Split-Trp assay of protein interaction*

Protein–protein interaction was assayed by the Split-Trp method essentially as described (O'Hare *et al.*, 2008). Briefly, *M. smegmatis* ΔHisA, a double auxotroph deficient in tryp-

tophan and histidine biosynthesis, was transformed with pairs of plasmids encoding $N_{trp}$-proteinA and proteinB-$C_{trp}$, where A and B were the test proteins, or unrelated control proteins. Transformants were grown on LB agar with the appropriate antibiotics. Each strain was cultured in liquid LB, washed with water, and then spotted onto Middlebrook 7H9 agar containing glucose (0.2%), glycerol (0.2%), Tween-80 (0.05%) and histidine (60 mg $l^{-1}$). Cells were also spotted in parallel onto LB agar containing the appropriate antibiotics, to check that each culture contained an equivalent number of viable bacteria. Plates were incubated at 25°C for 2–3 weeks and photographs shown are representative of three independent experiments.

### *GarA overexpression in* M. smegmatis

Electrocompetent *M. smegmatis* $mc^2155$ were transformed with 200 ng PL240 containing GarA, or a mutant of GarA, or no insert. After recovery in 2 ml of LB at 37°C for 4 h, cells were washed with water then 50 μl were spotted onto solid medium containing gentamicin (20 μg $ml^{-1}$). To test the effect of nutrient content, Middlebrook 7H9 broth was prepared according to a standard recipe (Difco) but omitting glutamate. The broth contains a nitrogen source (ammonium chloride), but no carbon source. Carbon sources were added at the following concentrations: amino acids at 3 mM (glutamate, glutamine, aspartate, alanine, arginine), other carbon sources at 10 mM (succinate, α-ketoglutarate, acetate) or 0.5% (glycerol, glucose). Plates were incubated at 37°C for 2–6 days and photographs shown are representative of three independent experiments.

### *Identification of the binding partners of GarA by affinity purification*

*Mycobacterium smegmatis* $mc^2155$ were grown in 1 l of Middlebrook 7H9 supplemented with glycerol 0.2%, glucose 0.2% and Tween-80 0.05% at 37°C until $OD_{600}$ 1.0. Cells were harvested and re-suspended in PBS with PMSF (1 mM). In parallel, two columns were charged with 300 μl of NiNTA agarose in PBS (Qiagen) then 300 μg of recombinant GarA was loaded onto one of the columns. Cell-free extract of *M. smegmatis* was prepared by sonication followed by centrifugation, and this extract was divided between the two columns. After extensive washing with PBS then PBS plus 0.05% Tween-20, proteins were eluted in 500 μl of PBS plus 200 mM imidazole. Eluted proteins were analysed by SDS-PAGE or used for assay of GDH activity. Cultures of *M. tuberculosis* H37Rv were also grown for purification of GarA binding partners. These were grown in 7H9 liquid medium supplemented with 10% v/v OADC (oleic acid, bovine serum albumin, D-glucose, catalase; Becton Dickinson). Cultures were grown at 37°C with shaking until $OD_{600}$ 1.0 then washed three times in PBS and harvested. Cell-free extracts were prepared by sonication, centrifugation and filtration, then processed as described above for extracts of *M. smegmatis*. For protein identification, proteins were excised from polyacrylamide gels, digested with trypsin and analysed using Ion Trap mass spectrometers HCT Ultra with ETD (Bruker Daltonics) and LTQ Linear Ion Trap (Thermo). The peptides identified by LC/MS/MS experiments were compared with databases of the *M. smegmatis* and *M. tuberculosis* H37Rv proteomes using Mascot (Matrix Science) and Phenyx (Genebio).

### *Assay of KGD activity in cell lysates*

Cultures of *M. smegmatis* were grown in 50 ml of 7H9 supplemented with glycerol 0.5%, glucose 0.5% and Tween-80 0.02% at 37°C until $OD_{600}$ 1.0. Cells were harvested and re-suspended in 50 mM potassium phosphate pH 6.5. Cells were disrupted by sonication and centrifuged to remove insoluble material. Total protein concentration was estimated by the Bradford assay. KGD assays contained 2 mM α-ketoglutarate, 0.3 mM TPP, 1 mM potassium hexacyanoferrate (III) and 1 mM $MgCl_2$ in 50 mM potassium phosphate pH 6.5. Assays were started by the addition of cell extract to 0.5 mg $ml^{-1}$ and the absorbance of ferricyanide was monitored at 425 nm. Assays were carried out at 25°C for 20 min. Background levels of ferricyanide reduction were recorded by omitting TPP or α-ketoglutarate. When required GarA was added at 1 μM. Parallel reactions used GarA phosphorylated by PknG or GarA phosphorylated by PknB.

### *Assay of recombinant KGD*

Reactions contained 0.1–3 mM α-ketoglutarate, 0.3 mM TPP, 1 mM potassium hexacyanoferrate (III) and 1 mM $MgCl_2$ in 50 mM potassium phosphate pH 6.5. Reactions were started by the addition of KGD and were incubated at 37°C. Initial rates were calculated during the linear phase of the reaction (20 min). When required, GarA was diluted in PBS and added to a final concentration of 5.7–833 nM. The rate of ferricyanide reduction was calculated based on the absorption coefficient of 1.02 $mM^{-1}$ $cm^{-1}$. To determine the $K_m$ for α-ketoglutarate, the concentration of KGD was 286 nM and the concentration of GarA was 0 or 2 μM. When measuring the concentration dependence of KGD inhibition by GarA, the concentration of KGD was 57 nM and α-ketoglutarate was 3 mM.

### *Assay of GDH activity using native protein*

Assay of GDH activity of affinity-purified proteins used NAD(P)H (1 mM), α-ketoglutarate 7.5 mM, ammonium chloride 50 mM, $MgCl_2$ 1 mM, in 50 mM HEPES pH 8.5. Eluted protein from the pull-down assay (1 mg $ml^{-1}$) was diluted five-fold into kinase buffer (20 mM HEPES pH 7.5, 20 mM $MgCl_2$, 5 mM $MnCl_2$) plus 100 μM ATP and incubated at 37°C for 30 min with 500 nM PknB, PknG or no kinase. Activity was then assayed with or without addition of further unphosphorylated GarA (1 μM). The absorption of NADH was measured at 340 nm and rates were calculated based on the absorption coefficient of 6.3 $M^{-1}$ $cm^{-1}$.

### *Assay of recombinant GDH*

The activity of GDH was measured by the change in absorbance at 340 nm due to production or consumption of NADH.

 

Reactions were performed in 50 mM HEPES pH 8.5 with 5 mM $MgCl_2$ and 1 mM $MnCl_2$. Reactions were started by the addition of 2 mM $NAD^+$ or 1 mM NADH and incubated at 37°C. To assay the effect of GarA on the oxidative deamination activity of GDH, reactions contained 68 nM GDH, 8–1200 mM glutamate and 0 or 2 μM GarA.

To assay the effect of GarA on the affinity of GDH for α-ketoglutarate, reactions contained 85 nM GDH, 50 mM ammonium chloride, 0.5–37.5 mM α-ketoglutarate and 0 or 2 μM GarA. The $K_m$ of GDH for ammonium was estimated using 85 nM GDH, 4 mM α-ketoglutarate and 2.5–100 mM ammonium chloride. The affinity of GarA for GDH was estimated using 85 nM GDH, 3 mM α-ketoglutarate, 50 mM ammonium chloride and 152–1140 nM GarA.

### *Determination of the site of phosphorylation of native GarA*

Aliquots (0.5 mg of protein) of cell-free extracts were prepared as described for affinity purification of GarA binding partners and used for phosphopeptide enrichment for MS. After trypsin digestion, phosphopeptides were purified using a $TiO_2$ column (Titansphere $TiO_2$ 5 μm, GL Sciences), desalted, and analysed using an ABI 4800 MALDI-TOF/TOF. Peptides were identified and the location of the phosphorylation site was determined by MS/MS.

## Acknowledgements

We thank Claudia Sala for culture of *M. tuberculosis* H37Rv and Simone Schmitt for help and advice. We are grateful to Diego Chiappe and Marc Moniatte of the Proteomics Core Facility, EPFL for protein identification. This work was supported by the European Commission [contract number LSHP-CT-2005-018923 (NM4TB) and a Marie Curie fellowship], and by PDT project 218/63 and PEDECIBA (Uruguay).

## References

Andersson, J.O., and Roger, A.J. (2003) Evolution of glutamate dehydrogenase genes: evidence for lateral gene transfer within and between prokaryotes and eukaryotes. *BMC Evol Biol* **3:** 14.

Belanger, A.E., and Hatfull, G.F. (1999) Exponential-phase glycogen recycling is essential for growth of *Mycobacterium smegmatis*. *J Bacteriol* **181:** 6670–6678.

van den Berg, S., Lofdahl, P.A., Hard, T., and Berglund, H. (2006) Improved solubility of TEV protease by directed evolution. *J Biotechnol* **121:** 291–298.

Boitel, B., Ortiz-Lombardía, M., Durán, R., Pompeo, F., Cole, S.T., Cerveñansky, C., *et al.* (2003) PknB kinase activity is regulated by phosphorylation in two Thr residues and dephosphorylation by PstP, the cognate phospho-Ser/Thr phosphatase, in *Mycobacterium tuberculosis*. *Mol Microbiol* **49:** 1493–1508.

Bormann, E.R., Eikmanns, B.J., and Sahm, H. (1992) Molecular analysis of the *Corynebacterium glutamicum gdh* gene encoding glutamate dehydrogenase. *Mol Microbiol* **6:** 317–326.

Bott, M. (2007) Offering surprises: TCA cycle regulation in *Corynebacterium glutamicum*. *Trends Microbiol* **15:** 417–425.

Brosch, R., Gordon, S.V., Garnier, T., Eiglmeier, K., Frigui, W., Valenti, P., *et al.* (2007) Genome plasticity of BCG and impact on vaccine efficacy. *Proc Natl Acad Sci USA* **104:** 5596–5601.

Camardella, L., Di Fraia, R., Antignani, A., Ciardiello, M.A., di Prisco, G., Coleman, J.K., *et al.* (2002) The Antarctic *Psychrobacter* sp. TAD1 has two cold-active glutamate dehydrogenases with different cofactor specificities. Characterisation of the $NAD^+$-dependent enzyme. *Comp Biochem Phys A* **131:** 559–567.

Canova, M.J., Veyron-Churlet, R., Zanella-Cleon, I., Cohen-Gonsaud, M., Cozzone, A.J., Becchi, M., *et al.* (2008) The *Mycobacterium tuberculosis* serine/threonine kinase PknL phosphorylates Rv2175c: mass spectrometric profiling of the activation loop phosphorylation sites and their role in the recruitment of Rv2175c. *Proteomics* **8:** 521–533.

Cowley, S., Ko, M., Pick, N., Chow, R., Downing, K.J., Gordhan, B.G., *et al.* (2004) The *Mycobacterium tuberculosis* protein serine/threonine kinase PknG is linked to cellular glutamate/glutamine levels and is important for growth *in vivo*. *Mol Microbiol* **52:** 1691–1702.

Cozzone, A.J. (2005) Role of protein phosphorylation on serine/threonine and tyrosine in the virulence of bacterial pathogens. *J Mol Microbiol Biotechnol* **9:** 198–213.

Durán, R., Villarino, A., Bellinzoni, M., Wehenkel, A., Fernandez, P., Boitel, B., *et al.* (2005) Conserved autophosphorylation pattern in activation loops and juxtamembrane regions of *Mycobacterium tuberculosis* Ser/Thr protein kinases. *Biochem Biophys Res Commun* **333:** 858–867.

Durocher, D., Taylor, I.A., Sarbassova, D., Haire, L.F., Westcott, S.L., Jackson, S.P., *et al.* (2000) The molecular basis of FHA domain: phosphopeptide binding specificity and implications for phospho-dependent signaling mechanisms. *Mol Cell* **6:** 1169–1182.

Fiuza, M., Canova, M.J., Zanella-Cléon, I., Becchi, M., Cozzone, A.J., Mateos, L.M., *et al.* (2008) From the characterization of the four serine/threonine protein kinases (PknA/B/G/L) of *Corynebacterium glutamicum* towards the role of PknA and PknB in cell division. *J Biol Chem* **283:** 18099–18112.

Garnak, M., and Reeves, H.C. (1979) Phosphorylation of Isocitrate dehydrogenase of *Escherichia coli*. *Science* **203:** 1111–1112.

Greenstein, A.E., Echols, N., Lombana, T.N., King, D.S., and Alber, T. (2007) Allosteric activation by dimerization of the PknD receptor Ser/Thr protein kinase from *Mycobacterium tuberculosis*. *J Biol Chem* **282:** 11427–11435.

Kawakami, R., Sakuraba, H., and Ohshima, T. (2007) Gene cloning and characterization of the very large NAD-dependent 1-glutamate dehydrogenase from the psychrophile *Janthinobacterium lividum*, isolated from cold soil. *J Bacteriol* **189:** 5626–5633.

Koul, A., Choidas, A., Tyagi, A.K., Drlica, K., Singh, Y., and Ullrich, A. (2001) Serine/threonine protein kinases PknF and PknG of *Mycobacterium tuberculosis*: characterization and localization. *Microbiology-SGM* **147:** 2307–2314.

Lu, C.D., and Abdelal, A.T. (2001) The *gdhB* gene of *Pseudomonas aeruginosa* encodes an arginine-inducible NAD(+)-dependent glutamate dehydrogenase which is

 

subject to allosteric regulation. *J Bacteriol* **183:** 490–499.
Mascher, T., Helmann, J.D., and Unden, G. (2006) Stimulus perception in bacterial signal-transducing histidine kinases. *Microbiol Mol Biol Rev* **70:** 910–938.
Minambres, B., Olivera, E.R., Jensen, R.A., and Luengo, J.M. (2000) A new class of glutamate dehydrogenases (GDH). Biochemical and genetic characterization of the first member, the AMP-requiring NAD-specific GDH of *Streptomyces clavuligerus*. *J Biol Chem* **275:** 39529–39542.
Müller, T., Strösser, J., Buchinger, S., Nolden, L., Wirtz, A., Krämer, R., and Burkovski, A. (2006) Mutation-induced metabolite pool alterations in *Corynebacterium glutamicum*: towards the identification of nitrogen control signals. *J Biotechnol* **126:** 440–453.
Munoz-Elias, E.J., and McKinney, J.D. (2006) Carbon metabolism of intracellular bacteria. *Cell Microbiol* **8:** 10–22.
Narayan, A., Sachdeva, P., Sharma, K., Saini, A.K., Tyagi, A.K., and Singh, Y. (2007) Serine threonine protein kinases of mycobacterial genus: phylogeny to function. *Physiol Genomics* **29:** 66–75.
Nguyen, L., Walburger, A., Houben, E., Koul, A., Muller, S., Morbitzer, M., *et al.* (2005) Role of protein kinase G in growth and glutamine metabolism of *Mycobacterium bovis* BCG. *J Bacteriol* **187:** 5852–5856.
Niebisch, A., Kabus, A., Schultz, C., Weil, B., and Bott, M. (2006) Corynebacterial protein kinase G controls 2-oxoglutarate dehydrogenase activity via the phosphorylation status of the OdhI protein. *J Biol Chem* **281:** 12300–12307.
O'Hare, H.M., Juillerat, A., Dianiskova, P., and Johnsson, K. (2008) A split-protein sensor for studying protein–protein interaction in mycobacteria. *J Microbiol Methods* **73:** 79–210.
Ortiz-Lombardía, M., Pompeo, F., Boitel, B., and Alzari, P.M. (2003) Crystal structure of the catalytic domain of the PknB serine/threonine kinase from *Mycobacterium tuberculosis*. *J Biol Chem* **278:** 13094–13100.
Pleissner, K.P., Eifert, T., Buettner, S., Schmidt, F., Boehme, M., Meyer, T.F., *et al.* (2004) Web-accessible proteome databases for microbial research. *Proteomics* **4:** 1305–1313.
Pullen, K.E., Ng, H.L., Sung, P.Y., Good, M.C., Smith, S.M., and Alber, T. (2004) An alternate conformation and a third metal in PstP/Ppp, the *M. tuberculosis* PP2C-family Ser/Thr protein phosphatase. *Structure* **12:** 1947–1954.
Scherr, N., Honnappa, S., Kunz, G., Mueller, P., Jayachandran, R., Winkler, F., *et al.* (2007) Structural basis for the specific inhibition of protein kinase G, a virulence factor of *Mycobacterium tuberculosis*. *Proc Natl Acad Sci USA* **104:** 12151–12156.
Schultz, C., Niebisch, A., Gebel, L., and Bott, M. (2007) Glutamate production by *Corynebacterium glutamicum*: dependence on the oxoglutarate dehydrogenase inhibitor protein OdhI and protein kinase PknG. *Appl Microbiol Biot* **76:** 691–700.
Senior, P.J. (1975) Regulation of nitrogen metabolism in *Escherichia coli* and *Klebsiella aerogenes*: studies with the continuous-culture technique. *J Bacteriol* **123:** 407–418.
Tafelmeyer, P., Johnsson, N., and Johnsson, K. (2004) Transforming a (beta/alpha)8-barrel enzyme into a split-protein sensor through directed evolution. *Chem Biol* **11:** 681–689.
Tian, J., Bryk, R., Itoh, M., Suematsu, M., and Nathan, C. (2005) Variant tricarboxylic acid cycle in *Mycobacterium tuberculosis*: identification of alpha-ketoglutarate decarboxylase. *Proc Natl Acad Sci USA* **102:** 10670–10675.
Usuda, Y., Tujimoto, N., Abe, C., Asakura, Y., Kimura, E., Kawahara, Y., *et al.* (1996) Molecular cloning of the *Corynebacterium glutamicum* ('*Brevibacterium lactofermentum*' AJ12036) *odhA* gene encoding a novel type of 2-oxoglutarate dehydrogenase. *Microbiology* **142:** 3347–3354.
Villarino, A., Durán, R., Wehenkel, A., Fernandez, P., England, P., Brodin, P., *et al.* (2005) Proteomic identification of *M. tuberculosis* protein kinase substrates: PknB recruits GarA, a FHA domain-containing protein, through activation loop-mediated interactions. *J Mol Biol* **350:** 953–963.
Walburger, A., Koul, A., Ferrari, G., Nguyen, L., Prescianotto-Baschong, C., Huygen, K., *et al.* (2004) Protein kinase G from pathogenic mycobacteria promotes survival within macrophages. *Science* **304:** 1800–1804.
Wang, R., Prince, J.T., and Marcotte, E.M. (2005) Mass spectrometry of the *M. smegmatis* proteome: protein expression levels correlate with function, operons, and codon bias. *Genome Res* **15:** 1118–1126.
Wehenkel, A., Bellinzoni, M., Graña, M., Durán, R., Villarino, A., Fernandez, P., *et al.* (2008) Mycobacterial Ser/Thr protein kinases and phosphatases: physiological roles and therapeutic potential. *Biochim Biophys Acta* **1784:** 193–202.
Young, T.A., Delagoutte, B., Endrizzi, J.A., Falick, A.M., and Alber, T. (2003) Structure of *Mycobacterium tuberculosis* PknB supports a universal activation mechanism for Ser/Thr protein kinases. *Nat Struct Biol* **10:** 168–174.

## Supporting information

Additional supporting information may be found in the online version of this article.

Please note: Wiley-Blackwell are not responsible for the content or functionality of any supporting materials supplied by the authors. Any queries (other than missing material) should be directed to the corresponding author for the article.

 